biology and life sciences forum

MDPI

Proceeding Paper

A Cytogenomic Analysis Reveals a New *Fusarium fujikuroi* Species Associated with Lemongrass (*Cymbopogon citratus*) †

Tomás Cavaco [1,*,‡], Catarina Gomes-Domingues [1,2,‡] and Filipe Gonçalves [1]

[1] Instituto Superior de Agronomia (ISA), Universidade de Lisboa, 1349-107 Lisboa, Portugal; catarinaagomes01@gmail.com (C.G.-D.); fpgonc@gmail.com (F.G.)
[2] Linking Landscape, Environment, Agriculture and Food (LEAF) Research Centre, Associated Laboratory TERRA, Instituto Superior de Agronomia (ISA), Universidade de Lisboa, Tapada da Ajuda, 1349-017 Lisboa, Portugal
* Correspondence: tomasfcavaco@gmail.com
† Presented at the 3rd International Electronic Conference on Agronomy, 15–30 October 2023; Available online: https://iecag2023.sciforum.net/.
‡ These authors contributed equally to the work.

Abstract: This study presents the first report of a *Fusarium* wilt in *Cymbopogon citratus* in Portugal. *Fusarium* is one of the most prominent genera of plant pathogens due to its wide range of hosts and mycotoxin production. The *Fusarium fujikuroi* species complex (FFSC) encompasses several threatening known plant pathogens. *Cymbopogon citratus* is a broadly distributed aromatic and medicinal plant rich in bioactive volatiles, which are relevant to several industries. The primary goal of this study was to identify and characterize the *Fusarium fujikuroi* species putatively responsible for the observed wilt. This report displays symptomatologic, cultural, morphologic, genetic, and cytogenomic characteristics associated with this fungus and disease. The cultural features included flat, white-colored colonies with filiform margins. Additionally, these colonies displayed abundant cottony aerial mycelia at the upper surface and orange-violet color at the lower surface. On Carnation Leaf-Piece Agar, septate fusoid macroconidia were present, displaying a flattened tapering toward the basal part and a number of septa ranging from one to four. The comparison between the amplified and aligned ITS sequences revealed 100% similarity between the isolate and the FFSC. Finally, a flow cytometry assay revealed an estimated genome size of 29.9 Mbp. This finding contrasts with other known pathogens from the *Fusarium fujikuroi* species complex. Ultimately, novel pathogens might be uncovered by exploring the mycobiome of diseased *Cymbopogon citratus* plants.

Keywords: Cytogenomics; lemongrass; fungal pathogen; *Fusarium fujikuroi* species complex; plant pathology

check for updates

Citation: Cavaco, T.; Gomes-Domingues, C.; Gonçalves, F. A Cytogenomic Analysis Reveals a New *Fusarium fujikuroi* Species Associated with Lemongrass (*Cymbopogon citratus*). *Biol. Life Sci. Forum* **2023**, *27*, 21. https://doi.org/10.3390/IECAG2023-15755

Academic Editor: Gianni Bellocchi

Published: 1 November 2023

1. Introduction

The *Fusarium* genus (Ascomycota: Hypocreales) is composed of ubiquitous filamentous fungi comprising 20 species complexes [1]. These ascomycetes are among the most economically relevant fungal plant pathogens, therefore being a threat to crop health and farmers' financial sustainability [2]. Furthermore, *Fusarium* spp. has secondary biosynthetic pathways capable of producing harmful mycotoxins, which lessens food safety worldwide [3]. The *Fusarium fujikuroi* species complex (FFSC) is divided into 3 distinct clades (American, African, and Asian), encompassing more than 50 different species [4]. Several causal agents of plant diseases belong to the FFSC, such as *Fusarium circinatum*, *F. fujikuroi*, *F. sacchari*, and *F. verticillioides*.

Cymbopogon citratus (DC.) Stapf (lemongrass) is a perennial, widely distributed aromatic and medicinal plant of the Poaceae family rich in secondary metabolites [5]. Most *C. citratus* cultivation is related to essential oil (EO) extraction since its volatiles have applications in the food, fragrance, and pharmaceutical industries [6]. The EO bioactivity is

related to its usual main compounds, namely, the monoterpene isomeric aldehyde mixture of neral and geranial, the monoterpene alcohol geraniol, and, less frequently, the monoterpene hydrocarbon β-myrcene [7]. This biological activity is greatly diversified, including bactericidal, insecticidal, fungicidal, and nematicidal activities [8–11]. Thus, *C. citratus* EO can be a great source of new biochemical biopesticides, which can justify an increasing demand for this crop.

In the present study, a preliminary first report of *C. citratus* wilt caused by an FFSC species in Portugal is described. Symptomatologic, cultural, morphologic, genetic, and cytogenomic characteristics associated with this pathogen and disease are displayed. Ultimately, by examining these various aspects, this work aims to gain a comprehensive understanding of the wilt and its causal agent.

2. Materials and Methods

2.1. Infected Plant Material and Isolation

The infected plants were observed and collected in a small organic garden (10 × 20 m) at Instituto Superior de Agronomia, Tapada da Ajuda, Portugal (38°42′46° N 9°11′04° W). The fungus was isolated from plant-infected tissues by cutting 5 pieces, each with approximately 2 cm^2, from the plant's collar in the transition zone between diseased and healthy tissue. Tissue pieces were then disinfected by immersing them in a NaClO solution (2% v/v) for 30 s, followed by double-rinsing in sterile distilled water to remove the disinfectant for 30 s each. After being washed and dried with sterile filter paper, the pieces were plated on potato dextrose agar (PDA, BD-Difco Laboratories, Detroit, MI, USA) supplemented with 250 mg/L chloramphenicol (BioChemica, AppiChem, Sauerlach, Germany). Inoculated Petri dishes were incubated at an inverted position at 25 °C and regularly checked (3–5 days) for the development of *Fusarium*-like fungi based on the cultural characteristics of colonies. After incubation, one isolate was selected and single-spored to obtain a monosporic culture. For this purpose, spores were diluted in sterile distilled water, and a drop of the suspension was spread on an agar medium using a platinum loop. Small agar blocks containing a single spore were cut under a microscope and transferred to new Petri dishes with PDA or malt extract agar (MEA, Oxoid, UK). Four replicates of this process were performed, two for each medium. Petri dishes were incubated for 7 days with a 12 h cycle of light or in complete darkness at 25 °C.

2.2. Cultural and Morphological Characterization

The isolate was characterized based on its cultural and morphological characteristics. Colony morphology, pigmentation, and type of aerial mycelium were determined on PDA and photographed using a Leica MZ12.5 stereomicroscope (Stuttgart, Germany) coupled with a Leica MC170 HD digital camera using the software Leica Application Suite (LAS) version 4.12.0 (Stuttgart, Germany). Morphological observations included the presence and characteristics of sporodochia; the size of sporodochial macroconidia and aerial microconidia; the shape and degree of septation of conidia; the disposition of the microconidia conidiophore branching patterns, and the presence or absence of chlamydospores, as previously described by Kamali-Sarvestani et al. [12]. These observations were made using a Leica DM 2500 microscope (Stuttgart, Germany) with differential interference contrast illumination, and the images were captured using a Leica DFC295 digital camera with the software Leica Application Suite (LAS) version 3.3.0. To induce the formation of sporodochia, agar blocks from single-spore cultures were placed in Petri dishes on Carnation Leaf-Piece Agar (CLA) following the method of the Fusarium Laboratory Manual [13].

2.3. DNA Extraction, PCR Amplification, and Sequencing

Total genomic DNA was extracted from mycelium grown in PDA plates adapting the Cenis protocol [14]. A 1.5 mL Eppendorf tube was filled with 500 µL of an Extraction Buffer (200 mM Tris HCl pH 8.5, 250 mM NaCl, 25 mM EDTA, 0.5% SDS) containing an

abrasive agent (100 µm glass beads), and a collected piece of mycelium was suspended. After macerating with a micro pestle and incubating for 10 min at 65 °C, the mycelial mat was pelleted via centrifugation for 1 min at 12,000 rpm. The supernatant was placed in a new tube; after measuring the collected volume, an equal volume of isopropanol was added, and after mixing by inverting the tubes, precipitated DNA was pelleted by centrifugation for 3 min at 12,000 rpm. After a wash with 300 µL of 70% ethanol and centrifuge for 1 min at 12,000 rpm, the pellet was vacuum-dried and resuspended in 50 µL of an Elution Buffer (10 mM Tris HCl pH 8.0, 1 mM EDTA). The primers V9G [15] and ITS4 [16] were used to amplify part of the nuclear rRNA operon (ITS) spanning the 3′ end of 18S rRNA gene, the first internal transcribed spacer, the 5.8S rRNA gene, the second ITS region, and the 5′ end of the 28S rRNA gene. PCR amplifications were performed using NZYTaq 2x Green Master Mix (Lisbon, Portugal), 1 µL of each primer (10 µM stock), and 1 µL of gDNA in a final volume of 20 µL. The cycle conditions in a T-gradient (Biometra, Göttingen, Germany) were 94 °C for 5 min, followed by 30 cycles at 94 °C for 30 s, 50 °C for 30 s, 72 °C for 30 s, and final elongation at 72 °C for 5 min. Verification of amplification was followed by performing agarose gel 1% electrophoresis, with DNA stained using GreenSafe (3 µL/100 mL gel) and visualized under UV light. Sequencing was performed by StabVida (Caparica, Portugal) using ITS4 primer. The sequence was edited using the UGENE program (Unipro, Novosibirsk, Russia) to remove ambiguous regions, and contigs assigned to the isolate were compared to the information available in the NCBI non-redundant nucleotide database.

2.4. Cytogenomic Analysis

Nuclear DNA content was estimated using flow cytometry. The preparation of suspensions of intact nuclei for analysis was performed following the method of Galbraith et al. [17]. The mycelium grown in PDA was chopped with a razor blade in a Petri dish containing 1 mL of a buffer (WPB 0.2 M Tris–HCl, 4 mM $MgCl_2$, 1% Triton X-100, Na_2EDTA 2 mM, NaCl 86 mM, sodium metabisulfite 20 mM, 1% PVP-10, pH 7.5; Loureiro et al. [18]). The nuclear suspension was sieved using a nylon mesh of 30 µm to remove large debris. Then, nuclei were stained with 25 µg mL^{-1} and a volume of 50 µL of propidium iodide (PI; Sigma-Aldrich, USA). To estimate the nuclear DNA content, DNA from *Colletotrichum acutatum* (C = 0.0689 pg; [19]) was used as the reference standard. The isolate's genome size was estimated by flow cytometry using a Partec CyFlow Space flow cytometer (Partec GmbH, Görlitz, Germany). The acquisition of numeric data and fluorescence graphs was performed using Sysmex FloMax software v2.4d (Sysmex, Görlitz, Germany), as described by Guilengue et al. [20]. The histograms for each sample were recorded, and the C-values were calculated with the following formula:

$$\text{Nuclear DNA Content (pg)} = (\text{Sample G1 Peak Mean} \times \text{GS of Reference Standard})/\text{Reference Standard G1 Peak Mean}$$

3. Results

3.1. Symptomatological Characteristics

Chlorotic spots on the leaves are the first symptoms of this disease that rapidly evolve into necrosis. Then, the collar region of the plant starts to necrose, followed by rot and wilt. Finally, the collar region is colonized by the pathogen mycelium, externally visible. Ultimately, generalized wilt affects the plant, and the collar region is severely rotted.

3.2. Cultural Characteristics

The cultural features in PDA included flat, white-colored colonies with filiform margins, abundant cottony aerial mycelia at the upper surface, and orange-violet color at the lower surface. The colony's appearance presented slight differences when incubated with a 12 h cycle of light or darkness, becoming dark brown at the center with age in the latter case. Additionally, isolates grew slightly less in dark conditions (Figure 1).

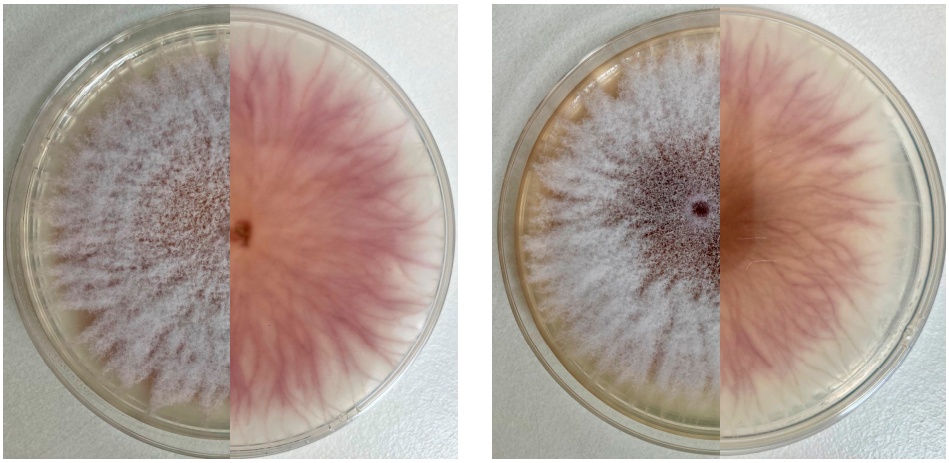

Figure 1. Isolate growth on PDA after seven days of incubation; (**a**) upper and reverse sides (from left to right) of a culture incubated with a 12 h cycle of light; (**b**) upper and reverse sides (from left to right) of a culture incubated in darkness.

3.3. Morphological Characteristics

On CLA, septate fusoid macroconidia were present, displaying a flattened tapering toward the basal part and a number of septa ranging from one to four; one-septate conidia: (12.3–)15.9–19.1(–22.7) × (3.0–)3.2–3.6(–3.8) µm (av. 17.5 × 3.4) µm; two-septate conidia: (18.4–)22.7–25.0(–28.2) × (3.0–)3.6–3.8(–4.4) µm (av. 23.8 × 3.7) µm; three-septate conidia: (26.2–)28.0–31.7(–38.1) × (3.3–)3.4–3.8(–4.2) µm (av. 30.3 × 3.7) µm; four-septate conidia: (35.3–)36.6–40.5(–45.4) × (3.5–)3.8–4.3(–4.6) µm (av. 39.1 × 4.1) µm. Microconidia were oval-shaped with a flattened basal, featuring zero septate or, rarely, one septate. They were formed on aerial conidiophores from monophialides, which may occur in V-shaped pairs suggesting a *rabbit ear* appearance. Conversely, aerial conidiophores were occasionally grouped in *false heads* but not found in chains. Aseptate microconidia: (5.4–)7.5–10.7 (–12.1) × (2.2–)2.4–3.2(–3.8) µm (av. 8.9 × 2.8) µm. Chlamydospores were absent. Other morphological features were found, such as anastomosis and *loop hyphae*. Anastomosis is a parasexual bridge found between macroconidia (Figure 2).

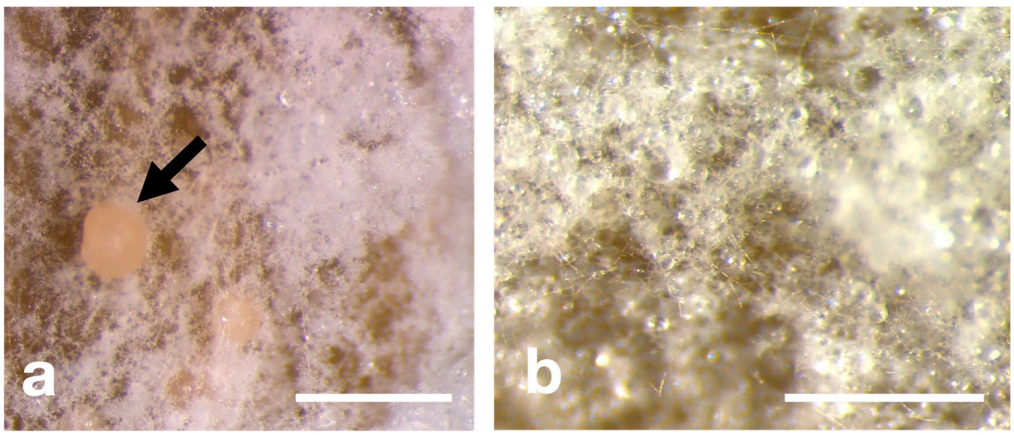

Figure 2. *Cont.*

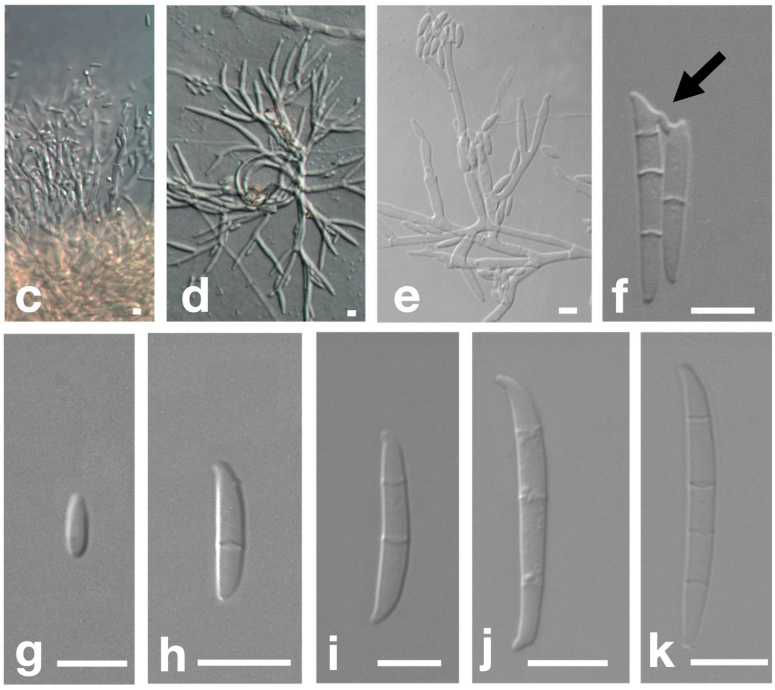

Figure 2. Morphological characteristics of the isolated *Fusarium* sp.; (**a**) sporodochia formed in CLA after 15 days of inoculation at 25 °C; (**b**) mycelium of a colonized leaf; (**c**) sporodochial conidiophore on CLA; (**d**) loop hyphae; (**e**) conidiophores with V-shaped pairs on aerial mycelium with aseptate microconidia; (**f**) anastomosis between macroconidia; (**g**–**k**) conidia with different numbers of septa. Scale bars: 1 mm (**a**,**b**), 10 µm (**c**–**k**).

3.4. Genetic Characteristics

A comparison of amplified and aligned sequences to the nucleotide NCBI database yielded 1157 results. Using the BLAST similarity search (performed on 15th March 2023), the ITS region of the ribosomal DNA region of the strain showed 100% (626/626 bp) similarity (with 0% gaps) to the FFSC. It was possible to infer about fungus phylogeny and identify it as an Ascomycete, belonging to the Pezizomycotina subdivision, Sordariomycetes class, Hypocreales order, Nectriaceae family, and the FFSC.

3.5. Cytogemonic Characteristics

The genome size reference used, *Colletotrichum acutatum*, has a nuclear DNA content of approximately 0.0689 pg [19]. Considering the output data from flow cytometry, displayed in Figure 3, the FFSC isolate displayed an estimated nuclear DNA content of about 0.0307 pg, which roughly corresponds to a genome size of 29.9 Mbp (Figure 3).

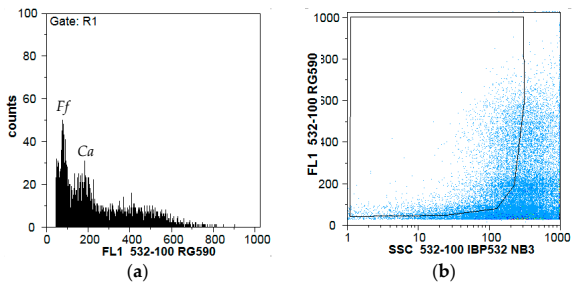

Figure 3. Genome-size measurement of the isolated fungus using flow cytometry; (**a**) histogram of relative fluorescence intensities of propidium iodide-stained nuclei simultaneously isolated from mycelium of FFSC isolate (*Ff*) and the DNA reference standard, *Colletotrichum acutatum* (*Ca*); (**b**) dot-plot of side light scatter (SSC) vs. fluorescence pulse integral in linear scale applying a gating region to exclude, as much as possible, partial nuclei and other debris to improve the quality of the histogram.

4. Discussion

Several diseases of *C. citratus* have a fungal etiology, comprising species from several genera, such as *Botrydiplodia*, *Curvularia*, *Fusarium*, *Helminthosporium*, *Pestalotiopsis*, *Puccinia*, *Rhyzoctonia*, *Tolyposporium*, and *Ustilago* [21,22]. Only *Fusarium equiseti* and *F. verticillium* have been associated with causing leaf spot and clump rot on *C. citratus* [21]. Neither of these species belongs to the FFSC, leading to the conclusion that the isolated pathogen cannot be one of these species, according to the nucleotide sequences of the ITS region. However, collar rot and wilt of *Cymbopogon winterianus*, java citronella, have been associated with *Fusarium verticillioides*, formerly known as *F. moniliforme*, which belongs to the FFSC [23,24]. Nevertheless, despite morphological similarities as monophialides in V-shaped pairs, *F. verticillioides* in CLA present numerous microconidial chains [24] that were not observed in the isolate. In addition, considering the cytogenomic data, which indicate that the isolated fungus has a genome size of approximately 29.9 Mbp, it is clear that the causal agent is not *Fusarium verticillioides*, which has a genome size of 42.4 Mbp [24]. Furthermore, *C. citratus* EO is capable of inhibiting the growth of *F. verticillioides* at in vitro bioassays, reinforcing the different etiology [25].

To the best of our knowledge, this is the first time that a fusariosis affecting *C. citratus* associated with a FFSC species has been described. A preliminary comprehensive characterization of the fungal causal agent was conducted, although some traits may be further studied.

In future research, other isolates will be collected, and more genome regions of this pathogen will be sequenced, such as TEF and RPB2 gene sequences. Likewise, the sequencing will include both forward and reverse directions using ITS1F or V9G and ITS4 primers to unveil the full identity of this *Fusarium* isolate. Additionally, Koch's postulates must be fulfilled to be sure of the pathogenicity of the isolate.

Author Contributions: Conceptualization, T.C., C.G.-D. and F.G.; formal analysis, T.C., C.G.-D. and F.G.; investigation, T.C., C.G.-D. and F.G.; data curation, C.G.-D.; writing—original draft preparation, T.C. and C.G.-D.; writing—review and editing, T.C., C.G.-D. and F.G. All authors have read and agreed to the published version of the manuscript.

Funding: This research received no external funding.

Institutional Review Board Statement: Not applicable.

Informed Consent Statement: Not applicable.

Data Availability Statement: The data is contained within the paper.

Acknowledgments: The authors would like to thank Ana Cabral for her invaluable assistance in this work, including laboratory support in cultural and morphological characterization and image acquisition. Similarly, the authors wish to thank Pedro Talhinhas for allowing the cytogenomic study of the isolate and Maria Odete Torres for supplying the original infected plant material. Additionally, the authors would like to thank Helena Oliveira for her memorable plant pathology classes. Finally, the authors wish to thank anonymous reviewers for their constructive feedback.

Conflicts of Interest: The authors declare no conflict of interest.

References

1. Ma, L.-J.; Geiser, D.M.; Proctor, R.H.; Rooney, A.P.; O'Donnell, K.; Trail, F.; Gardiner, D.M.; Manners, J.M.; Kazan, K. *Fusarium* Pathogenomics. *Annu. Rev. Microbiol.* **2013**, *67*, 399–416. [CrossRef] [PubMed]
2. Dean, R.; Van Kan, J.A.L.; Pretorius, Z.A.; Hammond-Kosack, K.E.; Di Pietro, A.; Spanu, P.D.; Rudd, J.J.; Dickman, M.; Kahmann, R.; Ellis, J. The Top 10 Fungal Pathogens in Molecular Plant Pathology. *Mol. Plant Pathol.* **2012**, *13*, 414–430. [CrossRef]
3. Chen, Y.; Kistler, H.C.; Ma, Z. *Fusarium graminearum* Trichothecene Mycotoxins: Biosynthesis, Regulation, and Management. *Annu. Rev. Phytopathol.* **2019**, *57*, 15–39. [CrossRef] [PubMed]
4. Niehaus, E.M.; Münsterkötter, M.; Proctor, R.H.; Brown, D.W.; Sharon, A.; Idan, Y.; Oren-Young, L.; Sieber, C.M.; Novák, O.; Pěnčík, A.; et al. Comparative "Omics" of the *Fusarium fujikuroi* Species Complex Highlights Differences in Genetic Potential and Metabolite Synthesis. *Genome Biol. Evol.* **2016**, *8*, 3574–3599. [CrossRef]
5. Lawal, O.A.; Ogundajo, A.L.; Avoseh, N.O.; Ogunwande, I.A. Cymbopogon citratus. In *Medicinal Spices and Vegetables from Africa*; Elsevier: Amsterdam, The Netherlands, 2017; pp. 397–423.

6. Majewska, E.; Kozlowska, M.; Gruszczynska-Sekowska, E.; Kowalska, D.; Tarnowska, K. Lemongrass (*Cymbopogon citratus*) Essential Oil: Extraction, Composition, Bioactivity and Uses for Food Preservation—A Review. *Pol. J. Food Nutr. Sci.* **2019**, *69*, 327–341. [CrossRef]
7. Akhila, A. *Essential Oil-Bearing Grasses: The Genus Cymbopogon*; CRC Press: Boca Raton, FL, USA, 2009; ISBN 0849378583.
8. Mayaud, L.; Carricajo, A.; Zhiri, A.; Aubert, G. Comparison of Bacteriostatic and Bactericidal Activity of 13 Essential Oils against Strains with Varying Sensitivity to Antibiotics. *Lett. Appl. Microbiol.* **2008**, *47*, 167–173. [CrossRef] [PubMed]
9. Aungtikun, J.; Soonwera, M.; Sittichok, S. Insecticidal Synergy of Essential Oils from *Cymbopogon citratus* (Stapf.), *Myristica fragrans* (Houtt.), and *Illicium verum* Hook. f. and Their Major Active Constituents. *Ind. Crops Prod.* **2021**, *164*, 113386. [CrossRef]
10. Lee, J.-E.; Seo, S.-M.; Huh, M.-J.; Lee, S.-C.; Park, I.-K. Reactive Oxygen Species Mediated-Antifungal Activity of Cinnamon Bark (*Cinnamomum verum*) and Lemongrass (*Cymbopogon citratus*) Essential Oils and Their Constituents against Two Phytopathogenic Fungi. *Pestic. Biochem. Physiol.* **2020**, *168*, 104644. [CrossRef]
11. Faria, J.M.S.; Cavaco, T.; Gonçalves, D.; Barbosa, P.; Teixeira, D.M.; Moiteiro, C.; Inácio, M.L. First Report on the Synergistic Interaction between Essential Oils against the Pinewood Nematode *Bursaphelenchus xylophilus*. *Plants* **2023**, *12*, 2438. [CrossRef]
12. Kamali-Sarvestani, S.; Mostowfizadeh-Ghalamfarsa, R.; Salmaninezhad, F.; Cacciola, S.O. *Fusarium* and *Neocosmospora* Species Associated with Rot of Cactaceae and Other Succulent Plants. *J. Fungi* **2022**, *8*, 364. [CrossRef]
13. Leslie, J.F.; Summerell, B.A. *The Fusarium Laboratory Manual*; John Wiley & Sons: Hoboken, NJ, USA, 2008; ISBN 0470276460.
14. Cenis, J.L. Rapid Extraction of Fungal DNA for PCR Amplification. *Nucleic Acids Res.* **1992**, *20*, 2380. [CrossRef]
15. De Hoog, G.S.; van den Ende, A.H.G.G. Molecular Diagnostics of Clinical Strains of Filamentous Basidiomycetes: Molekulare Diagnostik Klinischer Stämme Filamentöser Basidiomyzeten. *Mycoses* **1998**, *41*, 183–189. [CrossRef] [PubMed]
16. White, T.J.; Bruns, T.; Lee, S.; Taylor, J. Amplification and Direct Sequencing of Fungal Ribosomal RNA Genes for Phylogenetics. *PCR Protoc. Guide Methods Appl.* **1990**, *18*, 315–322.
17. Galbraith, D.W.; Harkins, K.R.; Maddox, J.M.; Ayres, N.M.; Sharma, D.P.; Firoozabady, E. Rapid Flow Cytometric Analysis of the Cell Cycle in Intact Plant Tissues. *Science* **1983**, *220*, 1049–1051. [CrossRef] [PubMed]
18. Loureiro, J.; Rodriguez, E.; Doležel, J.; Santos, C. Two New Nuclear Isolation Buffers for Plant DNA Flow Cytometry: A Test with 37 Species. *Ann. Bot.* **2007**, *100*, 875–888. [CrossRef] [PubMed]
19. Talhinhas, P.; Tavares, D.; Ramos, A.P.; Gonçalves, S.; Loureiro, J. Validation of Standards Suitable for Genome Size Estimation of Fungi. *J. Microbiol. Methods* **2017**, *142*, 76–78. [CrossRef]
20. Guilengue, N.; Alves, S.; Talhinhas, P.; Neves-Martins, J. Genetic and Genomic Diversity in a Tarwi (*Lupinus mutabilis* Sweet) Germplasm Collection and Adaptability to Mediterranean Climate Conditions. *Agronomy* **2019**, *10*, 21. [CrossRef]
21. Skaria, B.P.; Joy, P.P.; Mathew, S.; Mathew, G. 24—Lemongrass. In *Woodhead Publishing Series in Food Science, Technology and Nutrition*; Peter, K.V., Ed.; Woodhead Publishing: Sawston, UK, 2006; pp. 400–419. ISBN 978-1-84569-017-5.
22. Gardner, D.E. Lemongrass Rust Caused by *Puccinia nakanishikii* in Hawaii. *Plant Dis.* **1985**, *69*, 1100. [CrossRef]
23. Alam, M.; Chourasia, H.K.; Sattar, A.; Janardhanan, K.K. Collar Rot and Wilt: A New Disease of Java Citronella (*Cymbopogon winterianus*) Caused by *Fusarium moniliforme* Sheldon. *Plant Pathol.* **1994**, *43*, 1057–1061. [CrossRef]
24. Schoch, C.L.; Ciufo, S.; Domrachev, M.; Hotton, C.L.; Kannan, S.; Khovanskaya, R.; Leipe, D.; Mcveigh, R.; O'Neill, K.; Robbertse, B. NCBI Taxonomy: A Comprehensive Update on Curation, Resources and Tools. *Database* **2020**, *2020*, baaa062. [CrossRef] [PubMed]
25. Fandohan, P.; Gbenou, J.D.; Gnonlonfin, B.; Hell, K.; Marasas, W.F.O.; Wingfield, M.J. Effect of Essential Oils on the Growth of *Fusarium verticillioides* and Fumonisin Contamination in Corn. *J. Agric. Food Chem.* **2004**, *52*, 6824–6829. [CrossRef] [PubMed]